Using a HAP Network to Transfer WiMAX OFDM Signals: Outage Probability Analysis

Nicholas Vaiopoulos, Harilaos G. Sandalidis, and Dimitris Varoutas

***Abstract*—Transferring wireless broadband services across extremely far distances on Earth is usually implemented nowadays either by ground-based or satellite communications. Terrestrial networks require, however, heavy installation and maintenance costs, whereas satellite networks suffer from excessively high power requirements. An alternative but highly challenging solution is to employ a network consisting of high-altitude platforms (HAPs). In this paper, we propose a way of delivering WiMAX traffic using a serial multi-hop HAP network configuration. HAPs are located at specific locations in the stratosphere, pick up the traffic from the Earth region they cover, and communicate with each other using optical links. In such a configuration, we determine the WiMAX quality of service by evaluating the outage probability for the entire HAP network. The overall performance is examined by using a channel model that takes into account laser path loss and pointing error effects. The findings of the present study indicate that the consideration of specific network and channel model parameters is crucial toward the design and implementation of future multi-hop HAP networks.**

***Index Terms*—High altitude platform (HAP); Laser links; Multi-hop network; Outage probability; OFDM; WiMAX.**

I. Introduction

The rising demand for high-data-rate communication services has accelerated the need to develop new ways of data transmission. To this end, laser communications has started to attract considerable attention, since it provides a set of notable advantages over microwave transmission, including, among others, high bandwidth, intrinsic narrow beamwidth, communication privacy, small equipment size and weight, and no regulatory restrictions for frequency use [1]. These inherent characteristics have forced telecommunications research toward developing fully operative laser technologies for wide use in terrestrial and space applications. It is foreseen that in the next few years, laser communications will be a viable and reliable means of delivering data between ground stations, satellites, from Earth stations to satellites and vice versa, and between high-altitude platforms (HAPs) [2].

A HAP network is expected to be a challenging alternative to geostationary satellites regarding the seamless transfer of broadband services between distant places on Earth. HAPs combine some of the most distinctive characteristics of terrestrial wireless and satellite communication systems, e.g., broad service areas, great capacity, low transmission delay, adequate power consumption, etc. They are located in the stratosphere, approximately 25 km above the ground, and remain stationary, maintaining, thus, the same behavior as geostationary satellites. However, the short distances between HAPs and ground stations lead to lesser power demands and much smaller round-trip delays, making this technology quite attractive for broadband services in next-generation wireless communications [3]. Various research programs exploring the ability of carrying broadband data through wireless HAP links have been funded worldwide, e.g., Helios in the USA, CAPANINA and HAPCOS in Europe, SkyNet in Asia [4], etc. As such, several studies on HAP networks have appeared in the literature; see, e.g., [5], where a method of extending the capacity of HAP networks operating in the millimeter-wave bands is discussed.

HAPs may coexist with conventional wireless or optical networks to provide telecommunications services in remote geographical areas where terrestrial infrastructure is rather difficult and economically inefficient to deploy. Recent studies on coexistence scenarios focus mainly on WiMAX traffic delivery. Worldwide Interoperability for Microwave Access, commonly known as WiMAX, is a telecommunications technology based on the IEEE 802.16 standard and designed to provide affordable wireless broadband services using a variety of transmission modes. In general, WiMAX has affordable minimum implementation costs, can be readily deployed, and is more flexible than wired access technologies, such as digital subscriber lines, Ethernet, and fiber optics [6]. In [7] and [8], the authors investigated the performance and coexistence techniques for WiMAX delivered by HAPs and terrestrial systems in shared 5.75 and 3.5 GHz frequency bands, respectively. In [9], the performance of both downlink and uplink WiMAX broadband standard transmitted from

Manuscript received December 12, 2012; revised March 12, 2013; accepted May 8, 2013; published June 21, 2013 (Doc. ID 181679).

N. Vaiopoulos is with the Department of Informatics and Telecommunications, University of Athens, Panepistimiopolis, GR-15784 Athens, Greece, and with the Department of Computer Science and Biomedical Informatics, University of Central Greece, Papasiopoulou 2-4, Lamia GR-35100, Greece.

H. G. Sandalidis is with the Department of Computer Science and Biomedical Informatics, University of Central Greece, Papasiopoulou 2-4, Lamia GR-35100, Greece (e-mail: sandalidis@ucg.gr).

D. Varoutas is with the Department of Informatics and Telecommunications, University of Athens, Panepistimiopolis, Athens GR-15784, Greece.

http://dx.doi.org/10.1364/JOCN.5.000711

a HAP cellular system in the 3.5 GHz band across a coverage area of 30 km radius, operating in the same frequency band with terrestrial WiMAX deployments, is investigated. Finally, in [10], the communication system design and results of terrestrial and airborne pretrials for WiMAX payload developed for the Swiss-based HAP program "StratXX" are presented.

The requirement to deliver high amounts of transmission data between nodes in a HAP network is sufficiently confronted using laser technology. In terrestrial laser systems, radio signals can be securely transferred by using radio on free-space optics (RoFSO) technology. In this vein, Cvijetic and Wang in [11] proposed a terrestrial optical wireless overlay to transmit 802.16-2004 OFDM signals through multi-subcarrier modulation. In [12], the same authors presented a multi-input multi-output architecture for distributing IEEE 802.16d WiMAX traffic. A similar technology can be adopted for satellite or HAP networks. Arruego *et al.*, in [13], summarized the applications of optical wireless links to intra-spacecraft communications, together with their advantages, constraints, and the philosophy regarding their use in space. In [14], Fidler *et al.* provided a review of studies and experimental field trials for optical communications from and to HAPs, to transmit data at multi-gigabits per second, and discussed the pointing, acquisition, and tracking of laser terminals. Arnon, in [15], suggested a network configuration for WiMAX traffic delivery, including a satellite, several HAPS, and subscribers on the ground, and derived the laser transmitter (Tx) gain that minimizes the outage probability (OP) of the WiMAX link. In [16], the authors proposed a hybrid millimeter-wave/optical broadband HAP-to-ground backhaul link concept based on multiple HAP platforms.

In this paper, we present a novel HAP network architecture which aims at delivering WiMAX services across extremely far distances on Earth using multi-hop routing. HAPs in the network take the role of terrestrial base stations and collect the WiMAX traffic from the area they cover. They have transparent transponders that convert the WiMAX signals to optical signals and the reverse. The optical signals are transmitted from the source to the destination HAP through inter-HAP links and the traffic is delivered in this way to the end users after RF conversion. In such an architecture, we determine the WiMAX quality of service (QoS) by minimizing the OP for the network configuration. OP can be defined as the probability that the received power level is unacceptably low during a specified time duration. The overall performance is examined by using a channel model that incorporates laser path loss as well as pointing error effects.

The remaining sections of the paper are organized as follows. Section II summarizes the list of the variables and parameters used, for readers' convenience. In Section III, the network configuration, based on relayed HAPs, is discussed. Section IV examines a simple model of considering two HAPs. Specifically, we assume one-hop transmission and describe the optical Tx laser power, the pointing error model, and the optical receiver (Rx). Expressions for the electrical signal-to-noise ratio (SNR) are also deduced. Finally, the optimum half-beam divergence angle that minimizes the OP for one-hop transmission is derived. This optimum angle is used for the performance analysis in the multi-hop scenario presented in the next section. In Section V, novel analytical expressions of the end-to-end SNR statistics and OP for a multi-hop HAP network are provided, respectively. Proper WiMAX parameters are incorporated in order to make the model more realistic. Several numerical results to verify the accuracy of the derived expressions are presented using appropriate figures. Finally, some concluding remarks are given in Section VI.

II. Nomenclature

Next, we define for convenience most of the variables and parameters used throughout this paper:

- A_r: laser Rx aperture diameter.
- d_O: HAP-to-HAP distance.
- d_{RF}: distance between the destination HAP and the RF ground terminal.
- f_c: RF carrier frequency.
- F_N: noise figure of destination HAP RF amplifier.
- g_i: gain of the ith relay.
- $\sqrt{G_l}$: product of the destination HAP RF and ground terminal antenna field patterns in the line-of-sight direction.
- G_{R-O}: optical Rx telescope gain.
- G_{T-O}: optical Tx telescope gain.
- $h_{i,n}$: instantaneous intensity gain per subcarrier of the ith hop.
- $\mathcal{I}$: optical intensity.
- $\mathcal{I}_i$: pointing jitter-induced laser intensity at the ith hop.
- L: RF path loss.
- m: optical modulation index.
- m_n: optical modulation index per subcarrier.
- N: number of hops.
- N_{HAP}: pre-filtered AWGN.
- n_i: AWGN signal at the input of the ith relay.
- N_O: noise power density due to the HAP optical Rx.
- $N_{O,n}$: optical noise power per subcarrier.
- n_{opt}: filtered AWGN with a power spectral density of N_O.
- n_R: optics efficiency of the HAP optical Rx.
- n_T: optics efficiency of the HAP optical Tx.
- P_n: electrical signal power per subcarrier.
- $\mathcal{P}_{\mathrm{out,end}}$: OP over the OFDM band at the end user on Earth.
- $\mathcal{P}_{\mathrm{out,end},n}$: OP per subcarrier at the end user on Earth.
- $\mathcal{P}_{\mathrm{out},N}$: OP of the system after N hops.
- $\mathcal{P}_{\mathrm{out},N,n}$: OP per subcarrier after N hops.
- P_{R-O}: received optical power at the Rx.
- $P_{R-\mathrm{RF}}$: RF received power per subcarrier at RF ground Rx.
- P_{T-O}: transmitted optical power from the Tx.
- $P_{T-O\mathrm{av}}$: average transmitted optical power from the Tx.

- $P_{T-\mathrm{RF}}$: RF transmitted power per subcarrier from the destination HAP.
- $\mathcal{R}$: responsivity of the photodetector.
- R_i: ith optical transceiver.
- S: number of subcarriers in a channel.
- s_{OFDM}: OFDM signal for S subcarriers.
- T_s: OFDM symbol duration time.
- x_n: complex data symbol in the nth subcarrier.
- θ: laser half-beam divergence angle.
- λ_O: laser wavelength.
- λ_{RF}: wavelength of the RF signal.
- μ: instantaneous received electrical SNR per subcarrier.
- μ_{eq}: equivalent electrical SNR per subcarrier at the destination HAP Rx.
- μ_i: instantaneous electrical SNR per subcarrier of the ith hop
- $\mu_{\mathrm{RF}-R}$: received SNR per subcarrier at the RF ground terminal.
- $\mu_{\mathrm{RF}-R,\mathrm{th}}$: received SNR threshold per subcarrier at the RF ground terminal.
- $\mu_{\mathrm{RF}-T}$: RF SNR per subcarrier at the destination HAP RF.
- $\mu_{\mathrm{RF}-T,\mathrm{th}}$: RF SNR threshold per subcarrier at the destination HAP RF antenna.
- μ_{th}: electrical SNR threshold per subcarrier.
- σ^2: pointing jitter variance at the optical Rx.
- erfc(·): complementary error function [17, Eq. (7.1.2)].
- $\mathcal{L}^{-1}(\cdot)$: inverse Laplace transform.
- $\mathcal{M}_x(\sigma)$: MGF defined by $\int_0^\infty e^{\sigma x} f_x(x)\mathrm{d}x$.
- $W_{k,m}(\cdot)$: Whittaker function [17, Eq. (11.1.33)].

III. System Architecture

Figure 1 depicts a possible realization of the network architecture under consideration. More precisely, we consider a serial architecture where a HAP Tx, referred also in the manuscript as "source," communicates with the HAP Rx, referred as "destination," using intermediate HAPs acting as relays. The Tx collects the WiMAX traffic from heterogeneous networks on Earth. The WiMAX standard is based on orthogonal frequency-division multiplexing (OFDM) utilizing a large number of closely spaced orthogonal subcarriers [18]. OFDM belongs to multicarrier transmission schemes where high-data-rate streams are split into low-rate streams and then transmitted in parallel over a number of narrowband subcarriers [19]. In that way, a frequency selective channel is transformed into a number of flat fading subchannels. Each subcarrier is modulated with a conventional modulation format, e.g., M-QAM as considered in the present study. The total electrical power is available for transmission over the number of subcarriers, let us say S, in the WiMAX cell area served by the specific HAP. Modulation is implemented using the inverse fast Fourier transform, which assures orthogonality among all subcarriers over the symbol interval [20]. The RF OFDM signals modulate, then, the optical intensity of a laser diode. The optical signal from the output of the modulator is guided to the laser telescope, which transmits the optical beam through the channel using intensity-modulation/direct-detection (IM/DD) [21]. Figure 2(a) illustrates the block diagram of the OFDM laser Tx.

HAPs are located in space and communicate with each other assuming a Gaussian beam wave model. The inter-HAP channels are prone to extreme optical power attenuation while the wave propagates through space. Laser transmission also requires proper line-of-sight alignment between HAPs in order to have a viable communication link. This can be achieved through an appropriate pointing and tracking mechanism [6]. However, both mechanical vibrations and electronic noise cause the received spots from the laser beams to wander on the detector planes. Therefore, pointing error effects must be taken into account [22,23]. It has to be stressed that for typical inter-HAP distances of 100–200 km and HAP altitude of 25 km, the Rytov variance, which is a measure of turbulence severity, is quite small and hence scintillation effects have negligible effect and can be ignored.

The source HAP communicates with the destination HAP through $R_i, i = 1, 2, \ldots, N-1$ optical transceivers, which act as relay nodes all being in equidistance d_O, i.e., there are N point-to-point propagation links before the laser signals arrive at the destination. Relay assisted transmission is a common technique in wireless RF communication systems since it provides broader and more efficient coverage and can be used as a fading mitigation tool [24]. Every intermediate node in a multi-hop network acts as a router that forwards traffic toward its destination. That technique

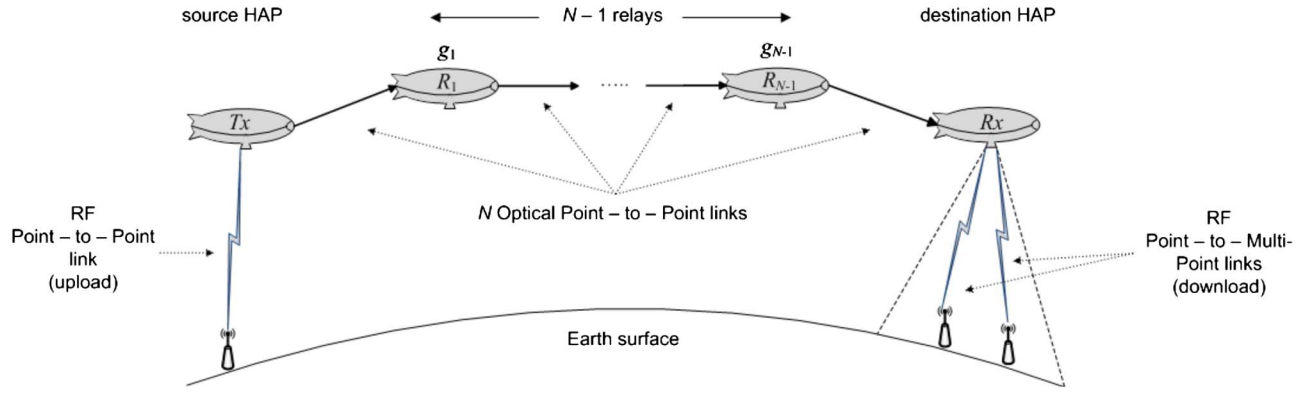

Fig. 1. HAP network configuration.

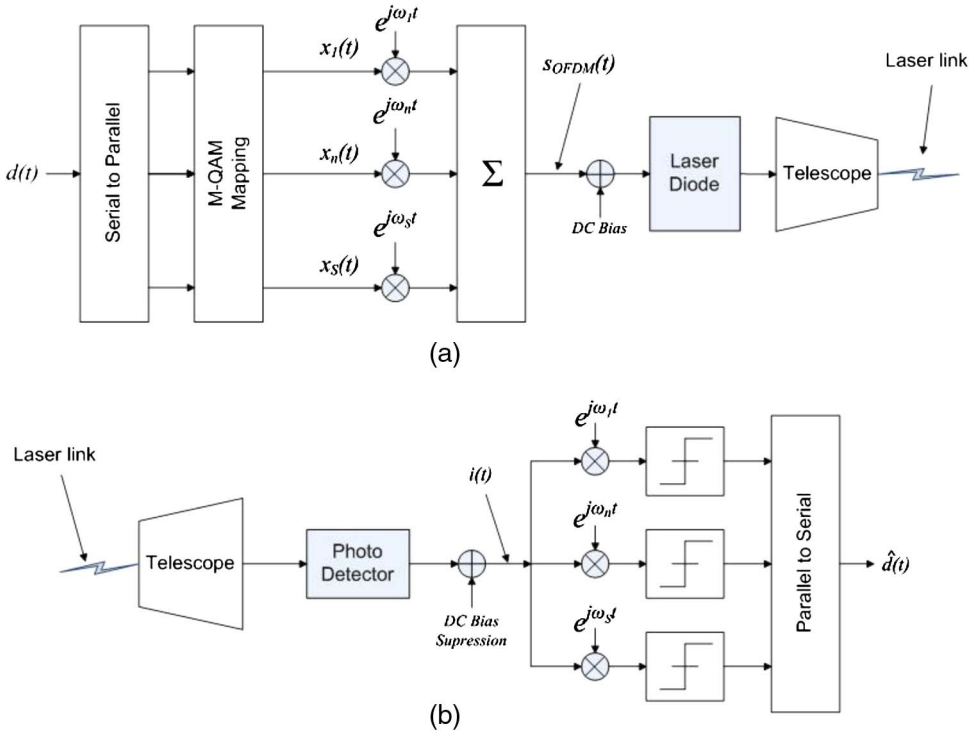

Fig. 2. Block diagram of (a) OFDM laser Tx and (b) OFDM laser Rx.

was also proposed to enhance terrestrial optical wireless transmission by mitigating various impairments, such as turbulence [25]. In the present study, we consider $N-1$ relays where each one has knowledge of the channel state of the previous hop. We assume the use of amplify-and-forward (AF) relays, which just amplify and forward the incoming signal without performing any sort of decoding. These relays use less complex circuitry compared to decode-and-forward (DF) relays, which decode the signal and then transmit the detected version to the destination HAPs [26].

The destination HAP receives the optical power using a telescope. Optical light can be concentrated by using lenses and mirrors, or any combination of them. A filter helps to remove the background radiation from entering the Rx, which generally creates shot noise and saturates the detector. The optical signal from the output of the filter propagates to the detector, which converts it to an RF electrical signal using a photodetector [27]. The orthogonality allows for efficient demodulator OFDM implementation using the fast Fourier transform at the Rx and requires no equalization [28]. Finally, the RF electrical signals are delivered to the end users located in the HAP Rx area. Figure 2(b) illustrates the basic configuration of the OFDM laser Rx.

IV. One-Hop Transmission Scenario

A. OFDM Laser Tx

In the simple one-hop transmission scenario, the source receives the OFDM WiMAX traffic from the ground. The OFDM signal in the RF domain, upon RF upconversion for S subcarriers, can be mathematically expressed by [21]

$$s_{\mathrm{OFDM}}(t)=\sum_{n=0}^{S-1}x_n\ \exp\left[j2\pi\left(\frac{n}{T_s}+f_c\right)t\right],\qquad 0\le tT_s. \quad (1)$$

By setting the guard interval to zero, the OFDM symbol duration, T_s, equals the Fourier analysis window [29].

The RF signal, $s_{\mathrm{OFDM}}(t)$, is used to modulate the optical intensity of a laser diode. In general, the nonlinear characteristic of the diode produces intermodulation terms that affect system performance. A model of such a diode was adopted in [30] where the optical output Y is expressed as a polynomial of the laser drive current X, i.e., $Y=C+A_1(X+A_2X^2+A_3X^3)$, where C, A_1, A_2, and A_3 are constants determined by the diode used. For a linear idealized diode, the laser is intensity modulated by an input current and emits optical power linearly related to the input current beyond a threshold lasing point. In that case, we do not consider possible harmonics generation and intermodulation distortions which are due to diode nonlinearity effects [16]. Hence, the constants A_2 and A_3 are zero and the optical laser power is proportional to the modulating signals [21,31] and can be written as

$$P_{T\text{-}O}(t)=P_{T\text{-}O\mathrm{av}}n_T G_{T\text{-}O}\times\left(1+\sum_{n=0}^{S-1}m_n x_n\ \exp\left[j2\pi\left(\frac{n}{T_s}+f_c\right)t\right]\right). \quad (2)$$

We further assume that all the tones are modulated with the same modulation index, m. Therefore, the above equation takes the following form:

$$P_{T\text{-}O}(t) = P_{T\text{-}O\text{av}} n_T G_{T\text{-}O}[1 + m s_{\text{OFDM}}(t)]. \quad (3)$$

B. Pointing Error Effects

Pointing errors have a severe effect on the link performance of a laser communications system operating at large distances. A well-known pointing error model for intersatellite laser links, used in many studies, dates back to the 1980s [32]. That model considers a negligible detector size with respect to the beam size at the Rx and it can be used for inter-HAP links, since HAPs are located at quite large distances. Tracking errors in the azimuth and elevation directions are modeled as independent and identically distributed zero-mean Gaussian random variables. Moreover, for negligible bias error angle from the center of the Gaussian beam, the probability density function (pdf) of the received optical intensity, $\mathcal{I}$, is shown to follow the beta distribution [33], i.e.,

$$f_{\mathcal{I}}(\mathcal{I}) = \beta \mathcal{I}^{\beta-1}, \qquad 0 \le \mathcal{I} \le 1, \quad (4)$$

where its average value is easily derived as

$$\bar{\mathcal{I}} = \frac{\beta}{\beta + 1}, \quad (5)$$

and β is a parameter given in terms of the pointing jitter and the half-beam divergence angle as

$$\beta = \frac{\theta^2}{4\sigma^2}. \quad (6)$$

C. OFDM Laser Rx

The optical power received by the photo detector in the Rx is described by the well known Friis transmission formula [27]:

$$P_{R\text{-}O}(t) = P_{T\text{-}O}(t) n_R G_{R\text{-}O} \left(\frac{\lambda_O}{4\pi d_O}\right)^2 \mathcal{I} + n_{\text{HAP}}(t). \quad (7)$$

The diode current, after noise filtering, can be expressed by substituting Eq. (2) into Eq. (7) as [21]

$$i(t) = \mathcal{R} n_T n_R G_{T\text{-}O} G_{R\text{-}O} P_{T\text{-}O\text{av}} \left(\frac{\lambda_O}{4\pi d_O}\right)^2 \mathcal{I} \times [1 + m s_{\text{OFDM}}(t)] + n_{\text{opt}}(t), \quad (8)$$

where the Gaussian noise, $n_{\text{opt}}(t)$, encompasses the dominant noise processes in the laser link, which is the sum of thermal noise, shot noise, and relative intensity noise processes with total noise power N_O. The shot noise is a function of the mean optical power; the relative intensity noise is a function of the square of the optical power, while the thermal noise is signal independent [34].

D. Electrical SNR Statistics

Taking Eq. (8) into account, we can deduce the desired signal power, P_n, per subcarrier as

$$P_n = m^2 \mathcal{R}^2 n_T^2 n_R^2 G_{T\text{-}O}^2 G_{R\text{-}O}^2 P_{T\text{-}O\text{av}}^2 \left(\frac{\lambda_O}{4\pi d_O}\right)^4 \mathcal{I}^2. \quad (9)$$

Moreover, the Tx and Rx telescope gain can be expressed according to [35] as

$$G_{T\text{-}O} = \frac{8}{\theta^2}, \quad (10)$$

$$G_{R\text{-}O} = \left(\frac{\pi A_r}{\lambda_O}\right)^2, \quad (11)$$

respectively.

Therefore, the instantaneous received electrical SNR, μ, per subcarrier can be defined statistically as a function of the expected desired signal power, P_n, and the optical noise power per subcarrier, $N_{O,n} = N_O/T_s$, as

$$\mu = \frac{m^2 \mathcal{R}^2 n_T^2 n_R^2 P_{T\text{-}O\text{av}}^2 \left(\frac{8}{\theta^2}\right)^2 \left(\frac{\pi A_r}{\lambda_O}\right)^4 \left(\frac{\lambda_O}{4\pi d_O}\right)^4 \mathcal{I}^2}{N_{O,n}}. \quad (12)$$

Equation (12) can be written as a function of the half-beam divergence angle θ, that is,

$$\mu = \frac{\alpha}{\theta^4} \mathcal{I}^2, \quad (13)$$

where

$$\alpha = \frac{m^2 \left(8 \mathcal{R} n_T n_R P_{T\text{-}O\text{av}} \left(\frac{A_r}{4 d_O}\right)^2\right)^2}{N_{O,n}}. \quad (14)$$

The pdf of electrical SNR, $f_\mu(\mu)$, can be easily derived from Eq. (4) after a simple power transformation of the random variable I as

$$f_\mu(\mu) = \frac{\beta}{2} \left(\frac{\alpha}{\theta^4}\right)^{-\frac{\beta}{2}} \mu^{\frac{\beta}{2}-1}, \qquad 0 \le \mu \le \frac{\alpha}{\theta^4}, \quad (15)$$

and can be given in a more concise form as

$$f_\mu(\mu) = \frac{\beta}{2} k^{-\frac{\beta}{2}} \mu^{\frac{\beta}{2}-1}, \qquad 0 \le \mu \le k, \quad (16)$$

where $k = \alpha/\theta^4$.

By following the definition, $F_\mu(\mu) = \int_0^\mu f_\mu(\mu) \mathrm{d}\mu$ and using Eq. (16), the cumulative distribution function of the instantaneous received electrical SNR is obtained as

$$F_\mu(\mu) = \left(\frac{\mu}{k}\right)^{\frac{\beta}{2}}, \qquad 0 \le \mu \le k. \quad (17)$$

E. Optimum Half-Beam Divergence Angle

The OP is defined as the probability that the instantaneous received electrical SNR falls below a specified threshold, μ_{th}, which represents a protection value of the SNR above which the quality of the channel is satisfactory. Then, the HAP-to-HAP OP per subcarrier can be expressed by

$$\mathcal{P}_{\text{out},1,n}(\mu_{\text{th}}) = \Pr(\mu < \mu_{\text{th}}) = F_{\mu}(\mu_{\text{th}}) = \left(\frac{\mu_{\text{th}}}{k}\right)^{\frac{\beta}{2}}, \quad 0 \le \mu_{\text{th}} \le k, \tag{18}$$

where the "1" in the index denotes the one-hop scenario.

Substituting Eq. (6) and the definition of k, we obtain

$$\mathcal{P}_{\text{out},1,n}(\theta, \mu_{\text{th}}) = \left(\sqrt{\frac{\mu_{\text{th}}}{\alpha}}\theta^2\right)^{\frac{\beta^2}{4\sigma^2}}, \qquad 0 \le \theta \le \left(\frac{\alpha}{\mu_{\text{th}}}\right)^{\frac{1}{4}}. \tag{19}$$

In order to evaluate the minimum OP, the laser half-beam divergence angle has to be calculated. By taking the derivative of Eq. (19) with respect to θ and setting it equal to zero, we readily find the value of θ_{opt} that minimizes the OP as

$$\theta_{\text{opt}} = \sqrt[4]{\frac{\alpha}{\mu_{\text{th}}}}\frac{1}{\sqrt{e}}. \tag{20}$$

That optimum angle is also used in all laser links for the multi-hop scenario presented in the next section. It must be noticed that when the number of subcarriers is large, the total OP over the entire OFDM band is derived based on the law of large numbers (LLN) as [21]

$$\mathcal{P}_{\text{out},1}(\mu_{\text{th}}) = \frac{1}{S}\sum_{n=0}^{S-1}\mathcal{P}_{\text{out},1,n}(\mu_{\text{th}}). \tag{21}$$

F. Numerical Results

In this section, we present some indicative numerical results for a typical set of parameter values, mainly adopted from [15,21,36], and [37], shown in Table I. It is mentioned that throughout the analysis these parameters are kept constant unless specified otherwise.

TABLE I
NUMERICAL PARAMETERS

Symbol	Value	Symbol	Value
A_r	0.3 m	n_T	0.9
d_{RF}	25 km	$\mathcal{R}$	0.8
d_O	120 km	$P_{T-O\text{av}}$	1 W
f_c	5 GHz	S	256
F_N	5 dB	SER	10^{-6}
$\sqrt{G_l}$	48.7 dB	T_s	0.1 μs
m	0.1	λ_O	1.55 μm
M	4	λ_{RF}	$6 \cdot 10^{-2}$ m
N	2	$\mu_{\text{RF}-T,\text{th}}$	14 dB
N_O	2×10^{-22} W/Hz	μ_{th}	50 dB
n_R	0.9	σ	8 μrad

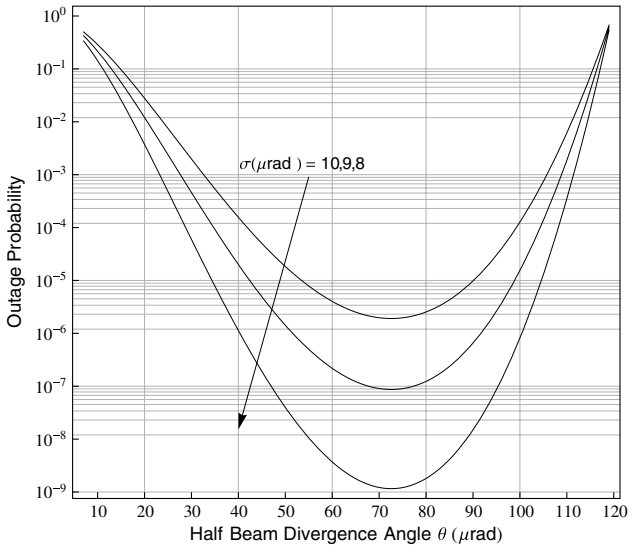

Fig. 3. One-hop OP versus HAP Tx half-beam divergence angle.

Figure 3 illustrates the one-hop OP against the half-beam divergence angle of the HAP Tx for various pointing jitter values. It is clear that the OP is minimized for a specific value of beam divergence angle (approximately 72 μrad) regardless the value of the pointing jitter. It also depicts the dominant effect of pointing jitter, e.g., an increment from 8 to 10 μrad induces a severe degradation of OP from 10^{-9} to 2×10^{-6} for a given value of beam divergence of 72 μrad.

To further investigate the impact of both the Tx half-beam divergence angle and electrical SNR threshold on the OP, we have produced the 3D plot of Fig. 4. We notice that, for a given θ, a decrease of the electrical SNR threshold leads to an improvement of the OP. Moreover, for a given value of the electrical SNR threshold a different

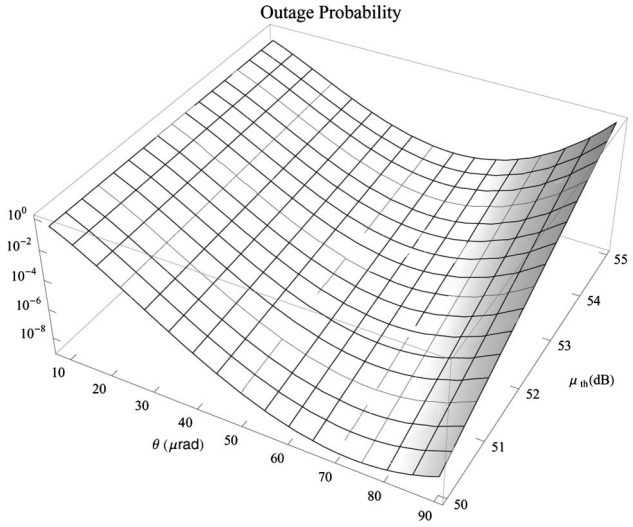

Fig. 4. One-hop OP versus HAP Tx half-beam divergence angle and electrical SNR threshold.

optimum value of beam divergence angle is obtained. That optimum value increases as the SNR threshold is reduced.

V. Multi-Hop Transmission Scenario

A. Electrical SNR at the Destination HAP

Considering a multi-hop network consisting of N hops between the source HAP and the destination HAP through $N-1$ nonregenerative relays, the received electrical signal per subcarrier at the final destination can be written as [38,39]

$$y_{N,n} = \prod_{i=1}^{N} g_{i-1} h_{i,n} x_n + \sum_{i=1}^{N} n_i \left(\prod_{t=i+1}^{N} g_{t-1} h_{t,n} \right), \qquad g_0 = 1, \tag{22}$$

where

$$h_{i,n} = m \mathcal{R} n_T n_R P_{T-O\text{av}} \left(\frac{8}{\theta^2} \right) \left(\frac{\pi A_r}{\lambda_O} \right)^2 \left(\frac{\lambda_O}{4\pi d_O} \right)^2 \mathcal{I}_i \tag{23}$$

denotes the instantaneous intensity gain per subcarrier of the ith hop. The optimum value of θ as previously derived, is assumed for every link. The equivalent SNR per subcarrier at the destination HAP Rx, μ_{eq}, can be written as [25]

$$\mu_{\text{eq}} = \frac{\prod_{i=1}^{N} h_i^2 g_{i-1}^2}{\sum_{i=1}^{N} N_{O,n} \left(\prod_{t=i+1}^{N} h_t^2 g_{t-1}^2 \right)}. \tag{24}$$

Setting the gain as the inverse of the fading state $g_i^2 = 1/h_i^2$, the relay just amplifies the incoming signal with the inverse of the channel of the previous hop, regardless of the noise of that hop. As mentioned in [38], such a kind of relay serves as a benchmark for all practical multi-hop
systems employing AF relays. When a multi-hop FSO system is employing AF relays, the equivalent electrical SNR at the destination HAP, assuming jitter independence among hops, can be extracted as

$$\mu_{\text{eq}} = \left(\sum_{i=1}^{N} \frac{1}{\mu_i} \right)^{-1}, \tag{25}$$

where

$$\mu_i = \frac{m^2 \mathcal{R}^2 n_T^2 n_R^2 P_{T-O\text{av}}^2 \left(\frac{8}{\theta^2} \right)^2 \left(\frac{\pi A_r}{\lambda_O} \right)^4 \left(\frac{\lambda_O}{4\pi d_O} \right)^4 \mathcal{I}_i^2}{N_{O,n}} = k \mathcal{I}_i^2 \tag{26}$$

is the instantaneous electrical SNR per subcarrier of the ith hop.

B. OP at the Destination HAP

The OP per subcarrier at the destination HAP can be expressed by [25]

$$\mathcal{P}_{\text{out},N,n}(\mu_{\text{th}}) = \Pr(\mu_{\text{eq}} < \mu_{\text{th}}) = \Pr\left(\frac{1}{\mu_{\text{eq}}} \geq \frac{1}{\mu_{\text{th}}} \right) = 1 - \mathcal{L}^{-1} \left(\frac{\mathcal{M}_{1/\mu_{\text{eq}}}(s)}{s} \right) \Big|_{s=1/\mu_{\text{th}}}. \tag{27}$$

From Eq. (25) and due to the independency of the jitter among hops, the $\mathcal{M}_{1/\mu_{\text{eq}}}(s)$ can be written as

$$\mathcal{M}_{1/\mu_{\text{eq}}}(s) = \prod_{i=1}^{N} \mathcal{M}_{1/\mu_i}(s). \tag{28}$$

Using also Eq. (16) and the definition of $1/\mu_i$, i.e., $\mathcal{M}_{1/\mu_i}(s) = \int_0^\infty e^{-s/x} f_{\mu_i}(x) \mathrm{d}x$, yields

$$\mathcal{M}_{1/\mu_i}(s) = \frac{\beta}{2} k^{-\frac{\beta}{2}} \int_0^k x^{\frac{\beta}{2}-1} e^{-s/x} \mathrm{d}x. \tag{29}$$

Hence, by applying [40, Eq. 3.471.2], Eq. (29) can be rewritten as

$$\mathcal{M}_{1/\mu_i}(s) = \frac{\beta}{2} k^{(1-\frac{\beta}{2})/2} s^{(\frac{\beta}{2}-1)/2} e^{-s/2k} W_{\frac{-1-\beta/2}{2}, \frac{\beta/2}{2}}(s/k). \tag{30}$$

By substituting Eq. (30) into Eq. (28), $\mathcal{M}_{1/\mu_{\text{eq}}}(s)$ is derived in closed form. Consequently, the OP given in Eq. (27) can be evaluated using any numerical method for the inverse Laplace transform.

C. OP at the Ground User

In this subsection, we consider the scenario where the destination HAP forwards the WiMAX traffic to the RF ground Rx. To this end, we incorporate the WiMAX parameters to our model in order to evaluate the performance of our network. The traffic in the destination HAP is converted in RF form and delivered to its footprint at the ground afterward. We adopt the following simplified model as a function of distance [36, Eq. 2.39]

$$P_{R-\text{RF}} = L P_{T-\text{RF}} = \left(\frac{\lambda_{\text{RF}} \sqrt{G_l}}{4\pi d_{\text{RF}}} \right)^2 P_{T-\text{RF}}. \tag{31}$$

RF transmission must satisfy both the required SNR for the service area size and the regulations set for each one of wireless services. By setting, thus, a required SNR value at the RF ground Rx station, $\mu_{\text{RF}-R}$, we can derive the appropriate transmitting power and hence the output SNR at the destination HAP RF antenna, $\mu_{\text{RF}-T}$. Taking into account the gain and noise figure F_N of the destination HAP RF antenna, we obtain the following relations between, μ_{eq}, $\mu_{\text{RF}-R}$, and, $\mu_{\text{RF}-T}$

$$\mu_{\text{RF}-T} = \frac{\mu_{\text{eq}}}{F_N}, \tag{32}$$

$$\mu_{\text{RF}-R} = L \mu_{\text{RF}-T}. \tag{33}$$

For a specific subcarrier there is typically a target minimum received SNR level $\mu_{\text{RF}-R,\text{th}}$, below which the

performance becomes unacceptable. From [36], the SNR threshold per subcarrier is obtained as

$$\mu_{\mathrm{RF}-R,\mathrm{th}} = \frac{2(M-1)}{3}\left(\mathrm{erfc}^{-1}\left(\frac{\mathrm{SER}}{2}\right)\right)^2. \tag{34}$$

In that case, the OP per subcarrier at the end user, $\mathcal{P}_{\mathrm{out,end},n}$, can be evaluated as

$$\begin{aligned}\mathcal{P}_{\mathrm{out,end},n} &= \Pr(\mu_{\mathrm{RF}-R} < \mu_{\mathrm{RF}-R,\mathrm{th}}) \\ &= \Pr(L\mu_{\mathrm{RF}-T} < \mu_{\mathrm{RF}-R,\mathrm{th}}) \\ &= \Pr\left(\frac{L\mu_{\mathrm{eq}}}{F_N} < \mu_{\mathrm{RF}-R,\mathrm{th}}\right) \\ &= \Pr\left(\mu_{\mathrm{eq}} < \frac{F_N}{L}\mu_{\mathrm{RF}-R,\mathrm{th}}\right) \\ &= P_{\mathrm{out},N,n}\left(\frac{F_N}{L}\mu_{\mathrm{RF}-R,\mathrm{th}}\right).\end{aligned} \tag{35}$$

For a large number of subcarriers, the OP over the OFDM band can be derived based on the LLN as

$$\mathcal{P}_{\mathrm{out,end}} = \frac{1}{S}\sum_{n=0}^{S-1}\mathcal{P}_{\mathrm{out,end},n}. \tag{36}$$

D. Performance Evaluation

We examine the performance evaluation of a multi-hop network using typical parameter values from Table I. In all simulations we used the optimum value of θ according to Eq. (20). In Fig. 5 we assume a multi-hop network of two hops and plot the OP versus the average received SNR per subcarrier for the ground Rx for several threshold values. It can be shown that a higher threshold leads to a worse OP performance for a given received SNR, as expected.

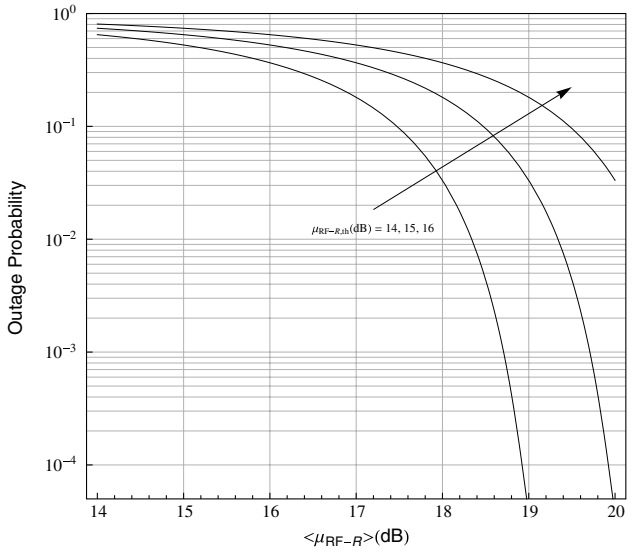

Fig. 5. OP versus the average received SNR per subcarrier for the ground Rx assuming two hops.

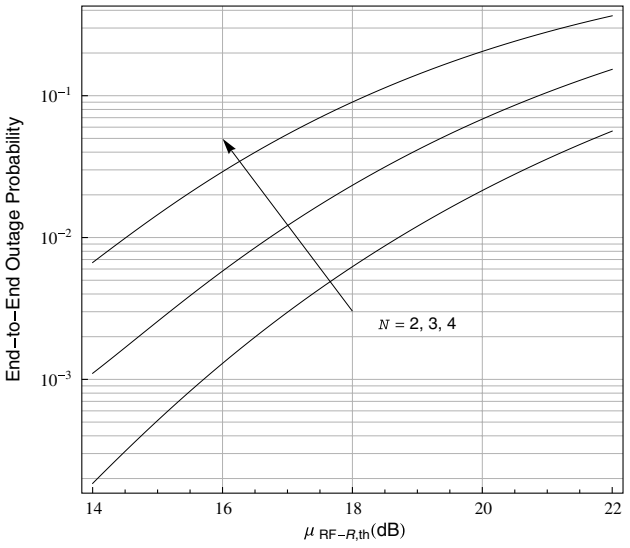

Fig. 6. OP at the ground Rx versus the SNR threshold at RF ground Rx for several hops.

Figure 6 presents the OP at the ground user against the SNR threshold on the Earth Rx in terms of the hop number N. It is assumed that the distance between the destination HAP and the ground Rx is constant and equals to 25 km. It is readily seen for low SNR threshold values that the transition from multi-hop operation through one to two relays degrades the OP by a factor equal to 10, whereas further exploitation of more relays (e.g., three relays or $N = 4$) reduces the OP by a factor equal to 6.

In Fig. 7, we study the impact of the distance between the HAP and the ground on the system performance. It is observed that, as the RF distance increases, the OP also rises since less power is delivered to the ground terminal. In addition, for a large number of hops the optical losses are greater and the OP at the ground terminal increases.

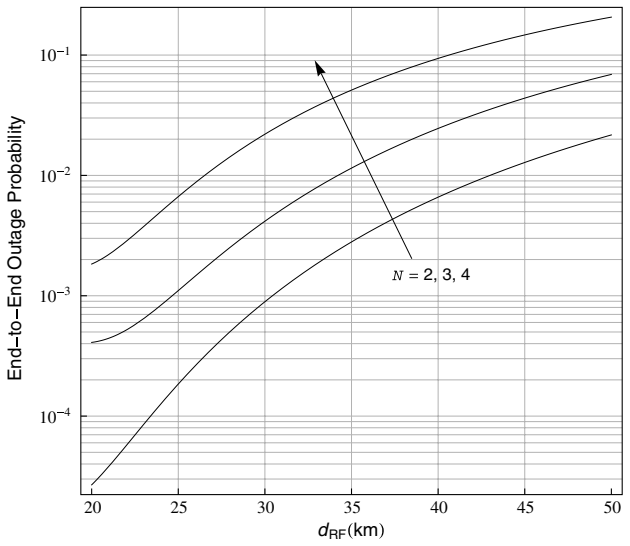

Fig. 7. OP at the ground Rx versus distance between the destination HAP and the RF ground Rx for various hops.

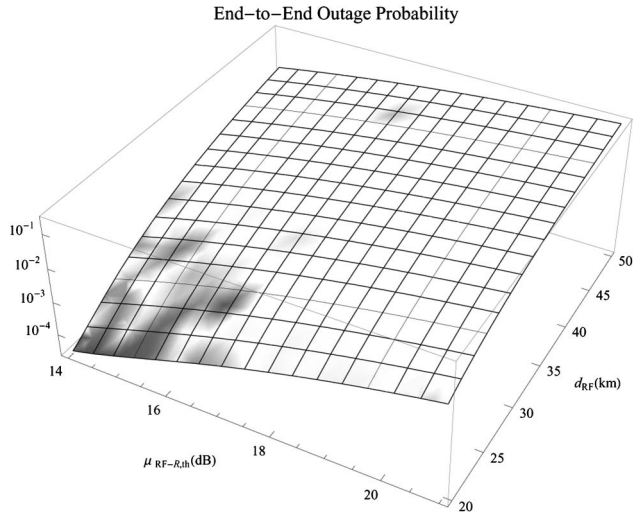

Fig. 8. OP at the ground Rx versus the SNR threshold at the RF ground Rx and distance between the destination HAP and the RF ground Rx.

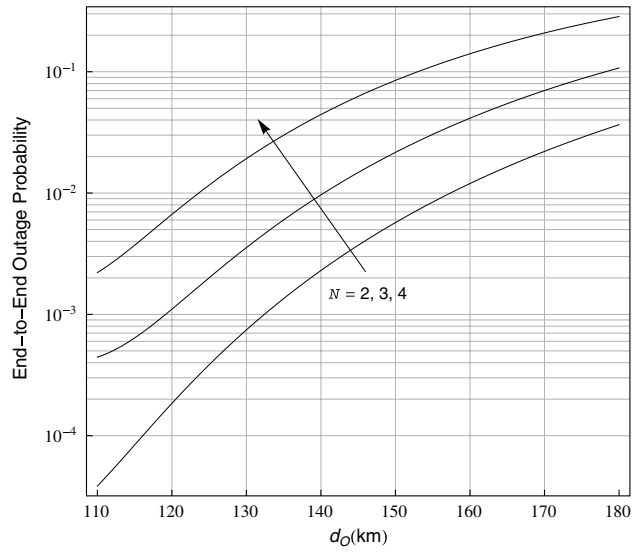

Fig. 9. OP at the ground Rx versus hop distance for several hops.

In Fig. 8, the OP is depicted against the SNR threshold at the ground Rx and the distance between the destination HAP and the Earth Rx. It is assumed that the number of hops N equals to 2. Apparently, the OP is getting high as either the SNR threshold or the distance increases.

Finally, in Fig. 9 the OP against the HAP-to-HAP distance for various hops N is presented. It can be seen that the OP grows as the HAP-to-HAP distance (keeping the number of hops constant) or the number of hops (keeping the HAP-to-HAP distance constant) increases.

VI. Conclusions and Further Research

In this paper, we presented an alternative method to deliver WiMAX services across extremely far distances on Earth by using a HAP network. A source HAP collects the traffic from the ground and communicates with the destination HAP using multi-hop routing through a number of intermediate HAPs. HAPs communicate with each other using laser links. After reaching the destination HAP, the traffic is transformed in RF form and delivered to the end users on Earth. The optical HAP transceiver and the laser inter-HAP channel, which takes into account the pointing error statistics, were analytically described. At first, we considered the case where the source directly communicates with the destination and then we generalized to a relayed scenario. We particularly focused on the OP at the ground users and presented proper graphical results for the performance evaluation of the network. The obtained results can serve as a guideline for designers to predict and evaluate a HAP network's ability to deliver broadband services in practice.

The analysis was conducted assuming a typical parameter set mainly used in practical systems. However, a thorough investigation is necessary in order to find the appropriate set for better performance. The choice, for example, of optimum gains and the beam divergence angle is a crucial point before the implementation process. Random angular jitter affects the overall performance and, therefore, proper tracking systems need to be considered. Throughout that study we assumed an inter-HAP distance of 150 km and $d_{RF} = 25$ km. At such altitudes and inter-HAP distances the Rytov variance is quite small, according to the Hufnagel–Valley model, leading to weak turbulence effects [1]. Therefore, turbulence has negligible effect and can be ignored. However, for larger HAP distances and different altitudes, turbulence may be severe and has to be taken into account. These are some of the issues that a designer needs to consider. Moreover, a technoeconomic study will shed light on the critical topic of cost deployment of a multi-hop HAP network.

The present analysis can be extended in a number of ways. For instance, it would be interesting to consider nonlinear laser diodes and examine the effect of intermodulation distortion, which is often present in practical laser links. Another extension is the consideration of turbulence in optical links for large inter-HAP distances. Fading may also be included in the RF downlink link. These additions would increase the mathematical complexity of the model but, on the other hand, make it much more reliable. Since practical HAP networks are currently working using microwave links, the idea of evaluating the performance of RF multi-hop links would be of particular help for comparison reasons. Moreover, different types of relays may be used, e.g., DF, all-optical relays, etc. Finally, the investigation of a coexistence scenario between heterogeneous HAP and satellite networks for increased overall performance appears quite challenging.

Acknowledgments

The authors would like to express their sincere thanks to Dr. Anna Mouti for her valuable comments helping improve the quality of the manuscript.

References

[1] L. Andrews and R. L. Philips, *Laser Beam Propagation Through Random Media*, 2nd ed. SPIE, 2005.

[2] D. G. Aviv, *Laser Space Communications*. Artech House, 2006.

[3] D. Grace and M. Mohorčič, *Broadband Communications via High Altitude Platforms*. Wiley, 2011.

[4] A. Aragón-Zavala, J. L. Cuevas-Ruíz, and J. A. Delgado-Penín, *High-Altitude Platforms for Wireless Communications*. Wiley, 2008.

[5] D. Grace, J. Thornton, G. Chen, G. White, and T. Tozer, "Improving system capacity of broadband services using multiple high altitude platforms," *IEEE Trans. Wireless Commun.*, vol. 4, no. 2, pp. 700–709, 2005.

[6] S. Ahson and M. Ilyas, *The WiMAX Handbook—Three-Volume Set*. CRC Press, 2008.

[7] P. Likitthanasate, D. Grace, and P. Mitchell, "Coexistence performance of high altitude platform and terrestrial systems sharing a common downlink WiMAX frequency band," *Electron. Lett.*, vol. 41, no. 15, pp. 858–860, 2005.

[8] Z. Yang, A. Mohammed, T. Hult, and D. Grace, "Downlink coexistence performance assessment and techniques for WiMAX services from high altitude platform and terrestrial deployments," *EURASIP J. Wireless Commun. Netw.*, vol. 2008, 291450, 2008.

[9] Z. Yang, A. Mohammed, and T. Hult, "Performance evaluation of WiMAX broadband from high altitude platform cellular system and terrestrial coexistence capability," *EURASIP J. Wireless Commun. Netw.*, vol. 2008, 348626, 2008.

[10] J. Thornton, A. D. White, and T. C. Tozer, "A WiMAX payload for high altitude platform experimental trials," *EURASIP J. Wireless Commun. Netw.*, vol. 2008, 498517, 2008.

[11] N. Cvijetic and T. Wang, "WiMAX over free-space optics-evaluating OFDM multi-subcarrier modulation in optical wireless channels," in *Proc. IEEE Sarnoff Symp.*, Princeton, NJ, Mar. 2006.

[12] N. Cvijetic and T. Wang, "A MIMO architecture for IEEE 802.16d (WiMAX) heterogeneous wireless access using optical wireless technology," in *Next Generation Teletraffic and Wired/Wireless Advanced Networking*. Springer-Verlag, 2006, pp. 441–451.

[13] I. Arruego, H. Guerrero, S. Rodriguez, J. Martinez-Oter, J. Jimenez, J. Dominguez, A. Martin-Ortega, J. de Mingo, J. Rivas, V. Apestigue, J. Sanchez, J. Iglesias, M. Alvarez, P. Gallego, J. Azcue, C. Ruiz de Galarreta, B. Martin, A. Alvarez-Herrero, M. Diaz-Michelena, I. Martin, F. Tamayo, M. Reina, M. Gutierrez, L. Sabau, and J. Torres, "OWLS: A ten-year history in optical wireless links for intra-satellite communications," *IEEE J. Sel. Areas Commun.*, vol. 27, no. 9, pp. 1599–1611, Dec. 2009.

[14] F. Fidler, M. Knapek, J. Horwath, and W. R. Leeb, "Optical communications for high-altitude platforms," *IEEE J. Sel. Topics Quantum Electron.*, vol. 16, no. 5, pp. 1058–1070, Sept.–Oct. 2010.

[15] S. Arnon, "Minimization of outage probability of WiMAX link supported by laser link between a high-altitude platform and a satellite," *J. Opt. Soc. Am. A*, vol. 26, no. 7, pp. 1545–1552, July 2009.

[16] D. Kedar, D. Grace, and S. Arnon, "Laser nonlinearity effects on optical broadband backhaul communication links," *IEEE Trans. Aerosp. Electron. Syst.*, vol. 46, no. 4, pp. 1797–1803, Oct. 2010.

[17] M. Abramovitz and I. A. Stegun, *Handbook of Mathematical Functions With Formulas, Graphs, and Mathematical Tables*, 9th ed. New York: Dover, 1972.

[18] M. Maqbool, M. Coupechoux, and P. Godlewski, "Comparison of various frequency reuse patterns for WiMAX networks with adaptive beamforming," in *Proc. of IEEE VTC Spring*, Marina Bay, Singapore, 2008.

[19] T. Ohtsuki, "Multiple-subcarrier modulation in optical wireless communications," *IEEE Commun. Mag.*, vol. 41, no. 3, pp. 74–79, Mar. 2003.

[20] J. Armstrong, "OFDM for optical communications," *J. Lightwave Technol.*, vol. 27, no. 3, pp. 189–204, Feb. 2009.

[21] A. Bekkali, C. B. Naila, K. Kazaura, K. Wakamori, and M. Matsumoto, "Transmission analysis of OFDM-based wireless services over turbulent radio-on-FSO links modeled by gamma-gamma distribution," *IEEE Photon. J.*, vol. 2, no. 3, pp. 510–520, June 2010.

[22] S. Arnon, "Optimization of urban optical wireless communications systems," *IEEE Trans. Wireless Commun.*, vol. 2, no. 4, pp. 626–629, July 2003.

[23] H. G. Sandalidis, "Optimization models for misalignment fading mitigation in optical wireless links," *IEEE Commun. Lett.*, vol. 12, no. 5, pp. 395–397, May 2008.

[24] M. Dohler and Y. Li, *Cooperative Communications: Hardware, Channel and PHY*. Wiley, 2010.

[25] G. K. Karagiannidis, T. A. Tsiftsis, and H. G. Sandalidis, "Outage probability of relayed free space optical communication systems," *Electron. Lett.*, vol. 42, no. 17, pp. 994–995, Aug. 2006.

[26] M. Uysal, Ed., *Cooperative Communications for Improved Wireless Network Transmission: Framework for Virtual Antenna Array Applications*. Information Science Reference, 2010.

[27] S. Arnon, "Optical wireless communications," in *Encyclopedia of Optical Engineering*, R. G. Driggers, C. Hoffman, and R. Driggers, Eds. CRC Press, 2003, pp. 1866–1886.

[28] R. V. Nee and R. Prasad, *OFDM for Wireless Multimedia Communications*. Artech House, 2000.

[29] W. Shieh and I. Djordjevic, *OFDM for Optical Communications*. Academic, 2010.

[30] J. C. Daly, "Fiber optic intermodulation distortion," *IEEE Trans. Commun.*, vol. 30, no. 8, pp. 1954–1958, Aug. 1982.

[31] W. Huang and M. Nakagawa, "Nonlinear effect of direct-sequence CDMA in optical transmission," in *IEEE Global Telecommunications Conference (GLOBECOM)*, Dubai, Nov. 18–20, 1994, pp. 1185–1189.

[32] C. Chen and C. S. Gardner, "Impact of random pointing and tracking errors on the design of coherent and incoherent optical intersatellite communication links," *IEEE Trans. Commun.*, vol. 37, no. 3, pp. 252–260, Mar. 1989.

[33] K. Kiasaleh, "On the probability density function of signal intensity in free-space optical communications systems impaired by pointing jitter and turbulence," *Opt. Eng.*, vol. 33, no. 11, pp. 3748–3757, Nov. 1994.

[34] H. Al-Raweshidy and E. S. Komaki, Eds., *Radio Over Fiber Technologies for Mobile Communication Networks*. Artech House, 2002.

[35] M. Toyoshima, T. Jono, K. Nakagawa, and A. Yamamoto, "Optimum divergence angle of a Gaussian beam wave in the presence of random jitter in free-space laser communication systems," *J. Opt. Soc. Am. A*, vol. 19, no. 3, pp. 567–571, Mar. 2002.

[36] A. Goldsmith, *Wireless Communications*. Cambridge University, 2005.

[37] A. Polishuk and S. Arnon, "Optimization of a laser satellite communication system with an optical preamplifier," *J. Opt. Soc. Am. A*, vol. 21, no. 7, pp. 1307–1315, July 2004.

[38] M. O. Hasna and M. S. Alouini, "Outage probability of multihop transmission over Nakagami fading channels," *IEEE Commun. Lett.*, vol. 7, no. 5, pp. 216–218, May 2003.

[39] G. K. Karagiannidis, T. A. Tsiftsis, and R. N. Mallik, "Bounds for multihop relayed communications in Nakagami-m fading," *IEEE Trans. Commun.*, vol. 54, no. 1, pp. 18–22, Jan. 2006.

[40] I. S. Gradshteyn and I. M. Ryzhik, *Table of Integrals, Series, and Products*, 7th ed. New York: Academic, 2008.

Nicholas Vaiopoulos was born in Lamia, Greece in July 1977. He received the B.Sc. degree in physics and the M.Sc. degree in electronics and radio communications in 2000 and 2003, respectively, both from the University of Athens, Greece. He is currently working toward the Ph.D. degree at the same University. Since 2009, he has been a member of the Special and Laboratorial Teaching Staff in the Department of Computer Science and Biomedical Informatics of the University of Central Greece. His major research interests include physical and MAC layer issues for fixed broadband wireless access systems and optical wireless communications. He serves as a reviewer for several journals and conferences.

Harilaos G. Sandalidis was born in Florina, Greece, in 1972. He received the five year Diploma degree in Electronics and Computer Engineering and the M.Sc. degree in Business Administration in the Production Engineering and Management Department from the Technical University of Crete, Greece, in 1995 and 1998, respectively. He also received the M.Sc. degree in Radiofrequency and Microwave Communications and the Ph.D. degree in the Telecommunications area at the Electronics and Telecommunications (former Electronics and Electrical Engineering) Department from the University of Bradford, UK, in 1996 and 2002, respectively. During the period between 1996 and 2001, he was a research assistant at the Telecommunications Systems Institute of Crete, Greece, working toward his Ph.D. degree in collaboration with Bradford University. After his military service, he joined TEMAGON, the technology consulting branch of the Hellenic Telecommunications Organization (OTE Group), in 2002, where he was involved in the risk mitigation program for the 2004 Olympic Telecommunication Network in collaboration with Telcordia Technologies, Inc. He also worked as a senior investigator at the Greek Ombudsman Office. In March 2009, he joined the University of Central Greece, where he is a Lecturer in the Department of Computer Science and Biomedical Informatics. His major research interests include optical wireless communications, computational intelligence, and heuristic optimization techniques regarding their application to the telecommunications field.

Dimitris Varoutas holds a Physics degree and M.Sc. and Ph.D. diplomas in communications and technoeconomics from the University of Athens. He serves as an assistant professor in the Department of Informatics and Telecommunications at the University of Athens. He has been participating in numerous European R&D projects in the RACE I & II, ACTS, Telematics, RISI, and IST frameworks in the areas of telecommunications and technoeconomics. He actively participates in several technoeconomic activities for telecommunications, networks, and services, such as the ICT-OMEGA and the CELTIC/CINEMA projects, as well as the Conferences on Telecommunications TechnoEconomics. He also participates in or manages related national activities for technoeconomic evaluation of broadband strategies, telecommunications demand forecasting, price modeling, etc. His research interests span design of optical and wireless communications systems to technoeconomic evaluation of network architectures and services. He has published more than 90 publications in refereed journals and conferences in the areas of telecommunications, optoelectronics, and technoeconomics, including leading IEEE journals and conferences. He is a Senior Member of Photonics (former LEOS), Communications, Education and Engineering Management Societies of IEEE and serves as a reviewer for several IEEE journals and conferences. Since 2007, he has been a Member of BOG of ADAE, the National Authority for Communications Security and Privacy.